

The crystallization kinetics of InF₃-based glass

J. MÁLEK*, Y. MESSADDEQ, S. INOUE, T. MITSUHASHI

National Institute for Research in Inorganic Materials, Namiki 1-1, Tsukuba, Ibaraki 305, Japan

The crystallization kinetics of (InF₃)₄₀(ZnF₂)₂₀(BaF₂)₁₅(SrF₂)₂₀(GdF₃)₂(LaF₃)₁(DyF₃)₂ glass was studied by differential scanning calorimetry. It was found that the two-parameter Šesták–Berggren equation gives a more quantitative description of the crystallization process than the Johnson–Mehl–Avrami model. The thermal stability criteria allowing comparison of different glass forming systems are discussed.

1. Introduction

The discovery of new fluoride glasses based on InF₃ has attracted increasing interest because they could extend the possibilities of the standard fluorozirconate glasses already in use [1]. Their extended infrared transmission range will allow the manufacture of optical fibres operating up to 5 μm, making possible the delivery of CO laser power [2]. Recently, much attention has been focused on active fibres for optical amplification [3]. It has been reported that the phonon energy in these glasses is lower than that in ZBLAN glass and the radiative quantum efficiency in the Pr³⁺-doped InF₃-based glass is approximately twice that of ZrF₄-based glass [4].

However, as applications of these glasses are centred upon optical fibres, it is necessary to investigate the crystallization kinetics in order to control nucleation and crystal growth during preform manufacturing and fibre drawing.

The aim of this work was to show a simple and reliable method of kinetic analysis of differential scanning calorimetry (DSC) data.

2. Theory

Usually it is assumed that the heat flow, Φ , generated during the crystallization process is directly proportional to the rate of the crystallization process ($d\alpha/dt$)

$$\Phi = \Delta H(d\alpha/dt) \quad (1)$$

ΔH being the enthalpy of the crystallization process. Assuming the Arrhenius rate constant $K(T) = A \exp(-E/RT)$, the kinetic equation is then expressed in the following form [5]

$$\Phi = \Delta H A e^{-x} f(\alpha) \quad (2)$$

where A is the pre-exponential factor and $x = E/RT$ is the reduced activation energy. The function $f(\alpha)$ represents the mathematical expression of the phenomenological kinetic model. The functions more fre-

quently used for the description of a crystallization process are summarized in Table I.

The aim of kinetic analysis of the crystallization process is to determine the best kinetic model providing the calculation of reliable kinetic parameters. It is well known, however, that the kinetic parameters A and E in the kinetic Equation 2 are mutually correlated [9, 10]. So it is practically impossible to determine all kinetic parameters by conventional non-linear regression algorithms of a single DSC curve. From this point of view it seems reasonable first to calculate the activation energy and then determine the kinetic model by the method described below.

The calculation of activation energy is based on a multiple-scan method in which several measurements performed at different heating rates, β , are needed. A very simple method was proposed by Friedman [11] for n th order reactions. However, it was made clear later [12–14] that this method is applicable to various processes. This expanded Friedman method follows from the logarithmic form of Equation 2

$$\ln \Phi = \ln[\Delta H A f(\alpha)] - \frac{E}{RT} \quad (3)$$

The activation energy is calculated from the slope of the plot of the logarithm of normalized heat flow at a given crystallization degree, plotted against the reciprocal temperature. Another method of calculation, known as the Kissinger's method [15], is based on the condition for the maximum for DSC peak

$$\ln \frac{\beta}{T_p^2} = \ln \frac{-f(\alpha_p)AR}{E} - \frac{E}{RT_p} \quad (4)$$

where T_p and α_p are the peak temperature and crystallization degree at the DSC peak, respectively, and β is the heating rate. The activation energy is then calculated from the slope of the $\ln(\beta/T_p^2)$ versus $1/T_p$ dependence. In fact, the first term on the right-hand side of Equation 4 is constant only for a first-order

* Permanent address: Joint Laboratory of Solid State Chemistry, Academy of Sciences of the Czech Republic, University of Pardubice, Studentská 84, Pardubice 530 09, Czech Republic.

TABLE I Kinetic models used for the description of the crystallization processes

Model		$f(\alpha)$
Johnson-Mehl-Avrami equation [6, 7]	(JMA)	$n(1 - \alpha)[- \ln(1 - \alpha)]^{1-1/n}$
Sestak-Berggren equation [8]	(SB)	$\alpha^m(1 - \alpha)^n$

process, i.e. $f(\alpha) = 1 - \alpha$, because in this case $f'(\alpha) = -1$. Nevertheless, it can be shown [16] that for other kinetic models the error in the activation energy determined by this method does not exceed 5%. If the activation energy is known, the kinetic model which best describes experimental DSC data can be found.

It is useful to define [9, 17] the function $z(\alpha)$ which can easily be obtained by a simple transformation of DSC data

$$z(\alpha) = \pi(x) \Phi T/\beta \quad (5)$$

where $\pi(x)$ is an approximation of the temperature integral which has to be introduced because Equation 2 cannot be integrated analytically. This approximation is usually expressed as a rational function and it is described in more detail elsewhere [18]. The simple Gorbachev's approximation [19], $\pi(x) = 1/(x + 2)$, is sufficiently accurate in many cases. The $z(\alpha)$ function is usually normalized within the $\langle 0, 1 \rangle$ interval and it always exhibits a maximum. It can be shown [9] that for the JMA model the maximum should be at $\alpha = 0.632$ within about 1% error and that it practically does not depend on the value of activation energy used for calculation of the $z(\alpha)$ function. (The maximum of the $z(\alpha)$ function should not be confused with the crystallization degree at the maximum of DSC peak α_p which, of course, strongly depends on E .) Therefore, the maximum of the $z(\alpha)$ function can be used as a very sensitive test of applicability of the JMA model. If the value is lower than 0.632, then the two-parameter SB model could be applied for the description of many crystallization processes.

Similarly, we can define the $y(\alpha)$ function [9, 20] which is again easily obtained by a simple transformation of DSC data

$$y(\alpha) = \Phi e^x \quad (6)$$

The maximum of this function α_M is confined to the interval $0 \leq \alpha_M < \alpha_p$ where α_p is crystallization degree at the maximum of DSC peak. The α_M value is important for the calculation of the kinetic exponent n (or m). If the kinetic model has been discriminated by the method described above, then the kinetic exponent can be calculated as given below.

2.1. The JMA model

If the function $y(\alpha)$ has a maximum at $\alpha_M > 0$ the kinetic exponent n can be calculated using the follow-

ing equation [9, 20]

$$n = \frac{1}{1 + \ln(1 - \alpha_M)} \quad (7)$$

If the maximum of the $y(\alpha)$ function is located at $\alpha_M = 0$, then the parameter n can be calculated by means of Šatava's method [21], from the slope of the plot of $\ln[- \ln(1 - \alpha)]$ versus $1/T$ which is nE/R . Another method of calculation of this parameter is based on the relationship derived from the condition for the maximum of the DSC peak [9]

$$n = \frac{1 - x_p \pi(x_p)}{\ln(1 - \alpha_p)} \quad (8)$$

Šatava's method usually gives slightly higher values of the kinetic exponent n than Equation 8. According to our experience [22], an average of these two values is a good approximation of the kinetic exponent.

2.2. The SB model

The ratio of the kinetic exponents m/n can be calculated from the maximum of the $y(\alpha)$ function [9]

$$m/n = \frac{\alpha_M}{1 - \alpha_M} \quad (9)$$

Equation 2 may be written in the following form

$$\ln(\Phi e^x) = \ln(\Delta H A) + n \ln[\alpha^{m/n}(1 - \alpha)] \quad (10)$$

The kinetic parameter n is then calculated [9] from the slope of linear dependence of $\ln(\Phi e^x)$ versus $\ln[\alpha^{m/n}(1 - \alpha)]$ plotted in the interval $\alpha \in (0.2, 0.8)$.

The pre-exponential factor is then calculated from the condition for the maximum of the DSC peak [9]

$$\ln A = x_p + \ln \frac{-\beta x_p}{T_p f'(\alpha_p)} \quad (11)$$

The consistency of the kinetic model applied is usually verified by testing the invariance of sets of kinetic parameters calculated for different scanning rates [9, 23].

3. Experimental procedure

The glass was prepared in a conventional way by melting, casting and annealing. The fluoride powders used to prepare the desired composition 40%InF₃, 20%ZnF₂, 15%BaF₂, 20%SrF₂, 2%GdF₃, 1%LaF₃, 2%DyF₃ (mol %) were mixed and heated at 700 °C for melting and then at 900 °C for refining. Then the melt was poured on to a brass mould preheated at the glass transition temperature, T_g .

The prepared glass was crushed into a powder and then sieved to particle size 420 μm. This powder was used for the crystallization kinetics measurements. Samples of about 10 mg were encapsulated in aluminium DSC pans and they were measured using a Perkin-Elmer DSC-7 instrument coupled with a 7700 Station. The instrument was previously calibrated with indium, lead and zinc standards. Non-isothermal DSC curves were obtained with selected heating rates (2–20 K min⁻¹) in the range from 100–500 °C. The kinetic analysis of the DSC data and

all calculations were performed by the TA-system software package [9].

4. Results and discussion

Typical DSC curves of the $(\text{InF}_3)_{40}(\text{ZnF}_2)_{20}(\text{BaF}_2)_{15}(\text{SrF}_2)_{20}(\text{GdF}_3)_2(\text{LaF}_3)_1(\text{DyF}_3)_2$ glass are shown in Fig. 1. The glass transition appears in the region 300–307 °C and it is associated with heat capacity change $\Delta C_p = 0.25 \pm 0.04 \text{ J g}^{-1} \text{ K}^{-1}$. There are various definitions of T_g . We prefer the integral method [24], where T_g is calculated as an intersection point of enthalpic curves for glass and undercooled liquid. The value of T_g determined in this way ($T_g = 305^\circ\text{C}$) depends only slightly on the heating rate and the standard deviation is lower than 2 °C.

The exothermal peaks observed in the DSC experiments correspond to the crystallization of several phases. The enthalpy of this crystallization process was determined to be $-\Delta H = 68 \pm 5 \text{ J g}^{-1}$. These non-isothermal DSC curves were used for calculation of kinetic parameters of the crystallization process. The values of the activation energy calculated by the Friedman method for different values of the crystallization degree are shown in Fig. 2. The dashed line

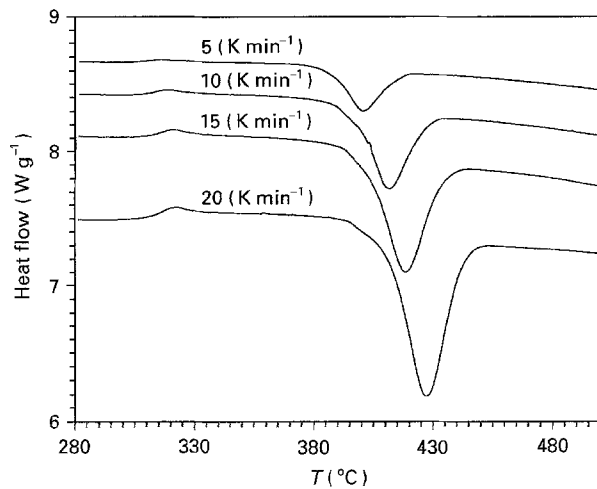


Figure 1 DSC curves of $(\text{InF}_3)_{40}(\text{ZnF}_2)_{20}(\text{BaF}_2)_{15}(\text{SrF}_2)_{20}(\text{GdF}_3)_2(\text{LaF}_3)_1(\text{DyF}_3)_2$ glass measured at different heating rates.

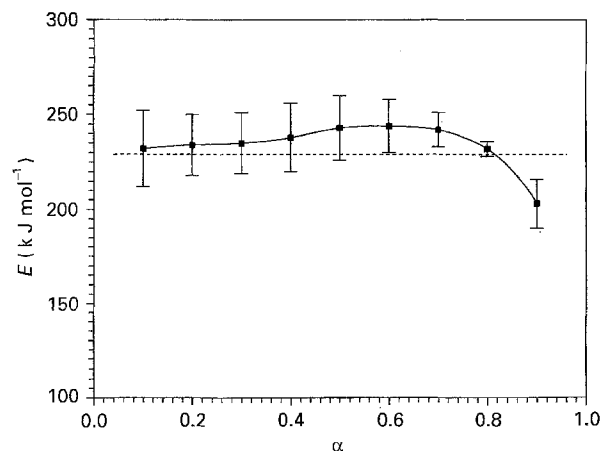


Figure 2 The values of the activation energy as a function of the crystallization degree: (■) calculated by the Friedman method; (---) the results of the Kissinger method.

corresponds to the value of activation energy determined by the Kissinger method. As is evident from the error bars, both methods give similar results within about 10% error.

Assuming that the value of activation energy of the crystallization process is $E = 229 \pm 20 \text{ kJ mol}^{-1}$, we can calculate both $y(\alpha)$ and $z(\alpha)$ functions using Equations 5 and 6. These functions normalized within the $\langle 0, 1 \rangle$ interval are shown in Fig. 3 for different heating rates (points). The maximum of the $z(\alpha)$ function is localized at $\alpha = 0.52 \pm 0.02$ and it is practically invariant with respect to the heating rate. It is clear that this value is considerably lower than 0.632, therefore the JMA model can hardly be used and the SB model seems to be more appropriate for the description of the crystallization process in the studied glass.

The maximum of the $y(\alpha)$ function was found to be $\alpha_M = 0.38 \pm 0.02$ and again it does not depend on the heating rate. The kinetic parameters calculated using Equations 7–11 are summarized in Table II for both kinetic models.

Fig. 4 shows experimental DSC data and curves calculated using kinetic parameters (see Table II) corresponding to the SB model and JMA model. The JMA model was derived for isothermal transformation conditions and it can only be applied if several additional assumptions are fulfilled [6, 7]. One of the

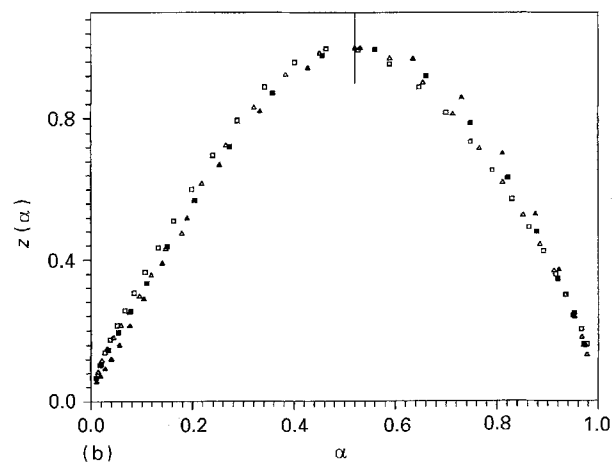
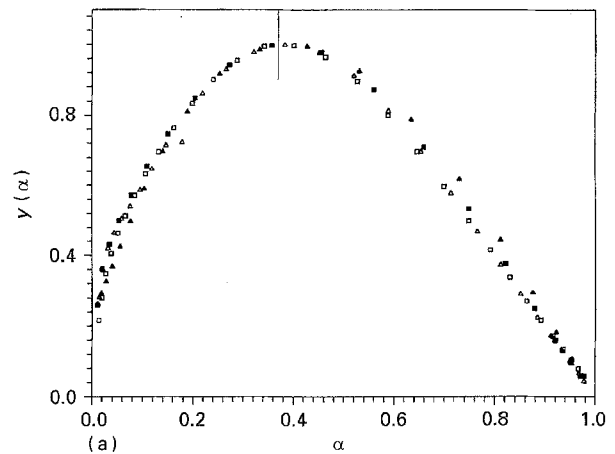


Figure 3 (a) Normalized $y(\alpha)$ function; (b) normalized $z(\alpha)$ function. Heating rate: (□) 5, (△) 10, (■) 15, (▲) 20 K min^{-1} . The points were calculated from Equations 5 and 6. The maxima are marked by line.

TABLE II The kinetic parameters of the crystallization process

Model	m	n	$E(\text{kJ mol}^{-1})$	$\ln A(\text{s}^{-1})$
SB	0.71 ± 0.03	1.16 ± 0.04	229 ± 20	36.0 ± 0.2
JMA	—	1.30 ± 0.05	229 ± 20	35.7 ± 0.2

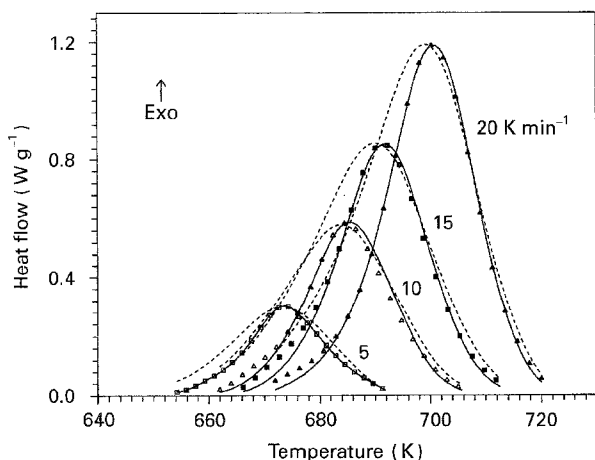


Figure 4 Experimental (points) and calculated DSC peaks corresponding to the crystallization process at various heating rates for (—) the SB model and (---) the JMA model. The kinetic parameters used for calculation are summarized in Table II.

most important assumptions is spatially random nucleation which limits the application of the JMA model to cases of homogeneous nucleation or heterogeneous nucleation at randomly dispersed nucleation centres. Another assumption is that the growth rate of a new phase depends only on temperature and not time. It was shown by Henderson [25] that the JMA equation can be applied in the non-isothermal conditions (e.g. DSC measurement) if the nucleation process takes place in early stages of transformation and the nucleation rate is zero thereafter. These criteria are evidently not fulfilled in this case because the DSC curve calculated for the JMA model is different in comparison with the experimental trace. It is evident that the SB model gives a better quantitative description of the crystallization process. The kinetic exponent m and n of the SB equation are linked with the mechanism of the crystallization process. Unfortunately, the link is still not clear. It was shown [26], however, that physically meaningful values of the parameter m should be confined to the interval $0 < m < 1$ which is fulfilled in this case.

The values of Arrhenius kinetic parameters, i.e. E and $\ln A$, are practically identical for both JMA and SB models (Table II). The value of the activation energy, E , obtained here is lower compared to IZBSC glasses [27]. There are two different mechanisms which can explain the activation energy of the crystallization process as obtained from DSC measurement. Melling and Uhlmann [28], have shown that for congruently melting glass-formers the crystal growth rate will be limited by the viscosity of the glass-forming liquid. In this case, E could be interpreted as the activation energy of viscous flow. Secondly, it is possible that the crystallization of complex glass-forming systems may be determined by processes at the melt-crystal interface. In this case, E corresponds to

the activation energy for the rate-limiting step. In many cases, linear growth kinetics is observed which is associated with diffusion-controlled crystal growth. To distinguish between these two mechanisms, further study is needed.

The kinetic parameters E and A are very important for the estimation of the thermal stability of glass (TSG). It has been proposed by Suriñach *et al.* [29] that the TSG could be estimated reasonably by calculating the Arrhenius crystallization rate constant at the glass transition temperature

$$\begin{aligned} \text{p}K(T_g) &= -\log(T_g) \\ &= 0.434(E/RT - \ln A) \end{aligned} \quad (12)$$

This criterion is very useful because it can be used to compare different glass-forming systems. However, in some cases it is not so easy to obtain reliable kinetic parameters E and $\ln A$, especially for the systems where multiple crystallization peaks are observed. For such cases it is more convenient to use the dimensionless criterion G defined [30] as

$$G = \frac{T_g - T_c}{\Delta H_\Sigma / C_p^*} \quad (13)$$

where T_c is the extrapolated onset of the crystallization peak, ΔH_Σ (J g^{-1}) is the total crystallization heat (corresponding to the sum of all crystallization peaks) and C_p^* is the heat capacity of undercooled melt. It can be estimated using the formula C_p^* ($\text{J g}^{-1} \text{K}^{-1}$) $\approx 28/M' + \Delta C_p$ where M' is the average molar weight of glass and ΔC_p (J g^{-1}) is the heat capacity change at T_g . All parameters needed to calculate G are obtained by a single DSC scan. It was shown recently [30, 31] that G is closely related to $\text{p}K(T_g)$ and so it can be considered as a good tool for estimating the thermal stability of glasses, especially when comparing various glass-forming systems. Another TSG criterion was introduced by Saad and Poulain [32]

$$S = (T_p - T_c)(T_c - T_g)/T_g \quad (14)$$

All these TSG criteria calculated for the $(\text{InF}_3)_{40}(\text{ZnF}_2)_{20}(\text{BaF}_2)_{15}(\text{SrF}_2)_{20}(\text{GdF}_3)_2(\text{LaF}_3)_1(\text{DyF}_3)_2$ glass are shown in Table III. The error limits shown in Table III correspond to the variation of thermal stability criteria with respect to the heating rate. It is evident that $\text{p}K(T_g)$ and G criteria are less sensitive to the heating rate than the criterion S . As criterion S is more influenced by experimental conditions, such as heating rate or sample mass, it often fails when one tries to compare different glass-forming systems. On the other hand, criteria $\text{p}K(T_g)$ and G allow direct comparison of the thermal stability of different glass-forming systems. From this point of view the thermal stability of the $(\text{InF}_3)_{40}(\text{ZnF}_2)_{20}(\text{BaF}_2)_{15}(\text{SrF}_2)_{20}(\text{GdF}_3)_2(\text{LaF}_3)_1(\text{DyF}_3)_2$ glass is comparable with binary chalcogenide glass of GeS_2 composition [30].

TABLE III Thermal stability criteria

$\text{p}K(T_g)$	4.7 ± 0.1
G	1.19 ± 0.05
S	4 ± 1

5. Conclusion

The kinetic analysis of the crystallization process of the $(\text{InF}_3)_{40}(\text{ZnF}_2)_{20}(\text{BaF}_2)_{15}(\text{SrF}_2)_{20}(\text{GdF}_3)_2-(\text{LaF}_3)_1(\text{DyF}_3)_2$ glass is presented. Several measurements at various heating rates provide a calculation of the activation energy and a very simple and convenient method of kinetic analysis enables us to determine the kinetic model of the crystallization process.

It was found that this crystallization process can be described by the two-parameter of Šesták–Berggren equation. The kinetic parameters calculated allow us to estimate the criterion of the thermal stability of glass.

Acknowledgement

Two authors (J. M. and Y. M.) thank the Science and Technology Agency of Japan for financial support. We also thank JISTEC and NIRIM for help with settlement in Japan.

References

1. Y. MESSADDEQ, PhD thesis, University of Rennes (1990).
2. Y. MESSADDEQ and M. POULAIN, *Mater. Sci. Forum* **67–68** (1991) 161.
3. T. SUGAWA, Y. NIYASIMA and T. KOMUKAI, *Elect. Lett.* **26** (1190) 2042.
4. Y. OHISHI, T. KANOMORI, T. NISHII, Y. NISHIDO and S. TAKAHASHI, in "Proceedings of the 16th Congress on Glasses", Madrid, Vol. 2 (1992) p. 76.
5. J. ŠESTÁK, "Thermophysical Properties of Solids, Their Measurements and Theoretical Analysis" (Elsevier, Amsterdam, 1984).
6. W. JOHNSON and R. MEHL, *Trans. Am. Inst. Min. Metall. Pet. Eng.* **135** (1939) 416.
7. M. AVRAMI, *J. Chem. Phys.* **9** (1941) 177.
8. J. ŠESTÁK and G. BERGGREN, *Thermochim. Acta* **3** (1971) 1.
9. J. MÁLEK, *ibid.* **200** (1992) 257.
10. J. MÁLEK and J. M. CRIADO, *ibid.* **203** (1992) 25.
11. H. L. FREIDMAN, *J. Polym. Sci.* **C6** (1964) 183.
12. T. OZAWA, *Thermochim. Acta* **31** (1986) 547.
13. *Idem. ibid.* **203** (1992) 159.
14. J. H. FLYNN and L. A. WALL, *J. Polym. Sci.* **B4** (1966) 323.
15. H. E. KISSINGER, *Anal. Chem.* **29** (1957) 1702.
16. J. M. CRIADO and A. ORTEGA, *J. Non-Cryst. Solids* **87** (1986) 302.
17. J. M. CRIADO, J. MÁLEK and A. ORTEGA, *Thermochim. Acta* **147** (1989) 377.
18. G. I. SENUM and R. T. YANG, *J. Therm. Anal.* **11** (1977) 445.
19. V. M. GORBACHEV, *ibid.* **13** (1978) 509.
20. J. MÁLEK, *Thermochim. Acta* **138** (1989) 337.
21. V. ŠATAVA, *ibid.* **2** (1971) 423.
22. J. MÁLEK, unpublished results.
23. J. MÁLEK, J. ŠESTÁK, F. ROUQUEROL, J. ROUQUEROL, J. M. CRIADO and A. ORTEGA, *J. Therm. Anal.* **38** (1992) 71.
24. M. J. RICHARDSON and N. G. SAVILL, *Polymer* **16** (1975) 753.
25. D. W. HENDERSON, *J. Non-Cryst. Solids* **30** (1979) 301.
26. J. MÁLEK, J. M. CRIADO, J. ŠESTÁK and J. MILITKÝ, *Thermochim. Acta* **153** (1989) 429.
27. Y. MESSADDEQ, A. DELBEN, M. AEGERTER and M. POULAIN, *Ceram. Trans.* **30** (1993) 303.
28. G. S. MELLING and D. R. UHLMANN, *Phys. Chem. Glasses* **2** (1967) 62.
29. S. SURINÁCH, M. D. BARO, M. T. CLAVAGUERA-MORA and N. CLAVAGUERA, *Fluid. Phase Equilib.* **20** (1985) 341.
30. J. MÁLEK, *J. Thermal. Anal.* **40** (1993) 159.
31. J. MÁLEK and L. TICHÝ, in "Trends in Non-Crystalline Solids", edited by A. Conde *et al.* (World Scientific, Singapore, 1992) p. 189.
32. M. SAAD and M. POULAIN, *Mater. Sci. Forum.* **19–20** (1987) 11.

Received 4 July 1994

and accepted 9 January 1995